HELIOS/3 beam request

CERN/SPSC 89-60
SPSC/R 92
October 12, 1989

MEMORANDUM

To: Prof. A.Donnachie, SPSC Chairman

From: Georges London, HELIOS/3 Spokesman

Copy: Reinhard Budde, SPSC Secretary; Rudiger Voss, SPS coordinator

The purpose of the HELIOS/3 experiment [SPSC/P240] is to measure low transverse mass dimuons in sulphur interactions as compared to proton interactions, both as a function of charged particle multiplicity in the same (forward) rapidity interval. The importance of the multiplicity dependence cannot be over-stressed: a quadratic dependence is one of the clearest indications of collective behavior such as a quark gluon plasma, thermalized or not [for example, R.C.Hwa and K.Kajantie, Phys.Rev. D32 (1985) 1109].

A first measure of this comparison in HELIOS/2 has been made and presented in our contribution to the Madrid conference [HELIOS NOTE 428, relevant part attached]. These *preliminary results give an upper limit at 90% confidence for anomalous sources in the low mass* region, $0.45 < M < 0.70$ GeV/c^2, of about 0.5 (1.4) of known sources for proton(sulphur)-Pt interactions, respectively. Comparing the two samples in the low mass region with the $\rho + \omega$ mass region, we can determine the fraction of dimuons produced with a quadratic multiplicity dependence in the low mass region; the upper limit, at 90% confidence, is 0.3-0.4. We are still studying our systematic errors. However, *the large statistical and systematic errors preclude a firm statement, in* particular on the upper limit of quadratic multiplicity dependence. These errors are related to the experimental setup of HELIOS which can be greatly improved.

Up to now, we have measured dimuons behind stacked Uranium calorimeters: a liquid argon calorimeter (ULAC), followed by two sets of U-scintillator calorimeters. This setup has three disadvantages:

1. a large amount of multiple scattering leading to a poorly reconstructed target resolution, leading to a difficult separation of target-produced and absorber-produced dimuons at low transverse mass, and a poor mass resolution which almost masks the $\rho + \omega$ meson production. *The background due to dimuons produced in the absorber is the most serious source of* systematic errors since it is hard to control.

2. an increase in the combinatorial background (i.e. π and K decays) in the empty spaces between the calorimeters, and

3. the time required to clear ULAC limited the beam intensity and thus the dimuon statistics.

In addition, in HELIOS/2, we measured the multiplicity dependence indirectly via the transverse energy deposited in the electromagnetic part of ULAC, whose rapidity coverage had almost no overlap with that of the muon spectrometer.

For the new experiment, we have determined an optimal configuration using the HELIOS muon spectrometer. We have optimized the absorber in two important ways:

- 6Λ of Al_2O_3 followed by 5Λ of Fe, improving the target and mass resolutions by a factor 2.5, and

- a hole in the absorber to force the projectile fragments to interact far from the target, followed by a tungsten rod to absorb the beam nonetheless.

Our new data acquisition system will enable us to increase the data-taking rate considerably. Most importantly, we will measure the multiplicity dependence directly, using silicon ring counters which will cover the muon acceptance.

We intend to measure directly the background due to absorber-produced dimuons by using hadron beams of different momenta impinging on the new absorber. For this measurement, we estimate from our Monte-Carlo simulation that we need to run 10 days at 100, 50 and 25 GeV/c, at 10^7 particles per burst with a negative beam. We will have sufficient statistics to be able to make a detailed comparison of the measured differential distributions with the Monte Carlo predictions, for example for the reconstructed target and mass. The overall normalization will also be established. In this way, we can "calibrate" and control our estimate of the absorber background.

From a detailed analysis [HELIOS note 429, attached] of the different sources of statistical and systematic errors in the present dimuon analysis, we conclude that we must compare the statistics of a 30 day sulphur run with that of a 30 day proton run. The latter comparison run will give us about 10% of the statistics of the sulphur run which, given the considerably smaller combinatorial subtraction, leads to similar errors. To reduce the systematic errors, the proton and sulphur runs must be compared in the same apparatus. In particular, the HELIOS/1 results using a low A target at 450 GeV/c, in a somewhat different kinematic region, can be compared to our results, but cannot be used to understand systematic errors.

The comparison of proton to sulphur data gives the largest lever arm on multiplicity, considerably larger than the comparison between low E_T and high E_T in the sulphur data even after the normalization to the number of projectile participants. In the note 429, we show that the best treatment of the systematic errors comes from a comparison of the lowest mass region to the $\rho + \omega$ region for **both proton and sulphur data.** We are presently limited by statistics, a bad mass resolution and the knowledge of the absorber subtraction.

In summary, we wish to request 14 days for setting-up, 10 days for background studies and 30 days for proton comparison running, or a total of 54 days, summarized in the Table. We request 2 days of setting-up early in the fixed-target period to check the new absorber for alignment and punchthrough, and the remaining just before the sulphur running. We expect that the latter run will be near the end of the fixed-target period, but not necessarily at the end.

Since we are in the same beam-line as the NA45 experiment which will be setting up, we are concerned about loss of beam time due to frequent access after we begin to take data; we request that these accesses be kept to a strict minimum.

We firmly believe that, with sufficient proton and sulphur data in 1990, we can give at the beginning of 1991 a quantitative estimate of the amount of collective behavior in sulphur-nucleus interactions relative to proton-nucleus interactions, and thus be able to make a judgment of the interest of ultra-relativistic nuclear beams. HELIOS/3 is the only experiment which can rapidly and directly answer this crucial question using dileptons.

Table 1: SUMMARY OF NA34/3 REQUEST

	beam	momentum	days
setting up			14
background studies	negative	25–100 GeV/c	10
proton comparison	proton	200 GeV/c	30
sulphur	Sulphur	200 GeV/u	30

HELIOS note 12?

27.9.1989

Georges LONDON

only pp part

Comprehensive results on nucleus – nucleus interactions at 200 GeV/nucleon

HELIOS COLLABORATION

MADRID contribution V – 14

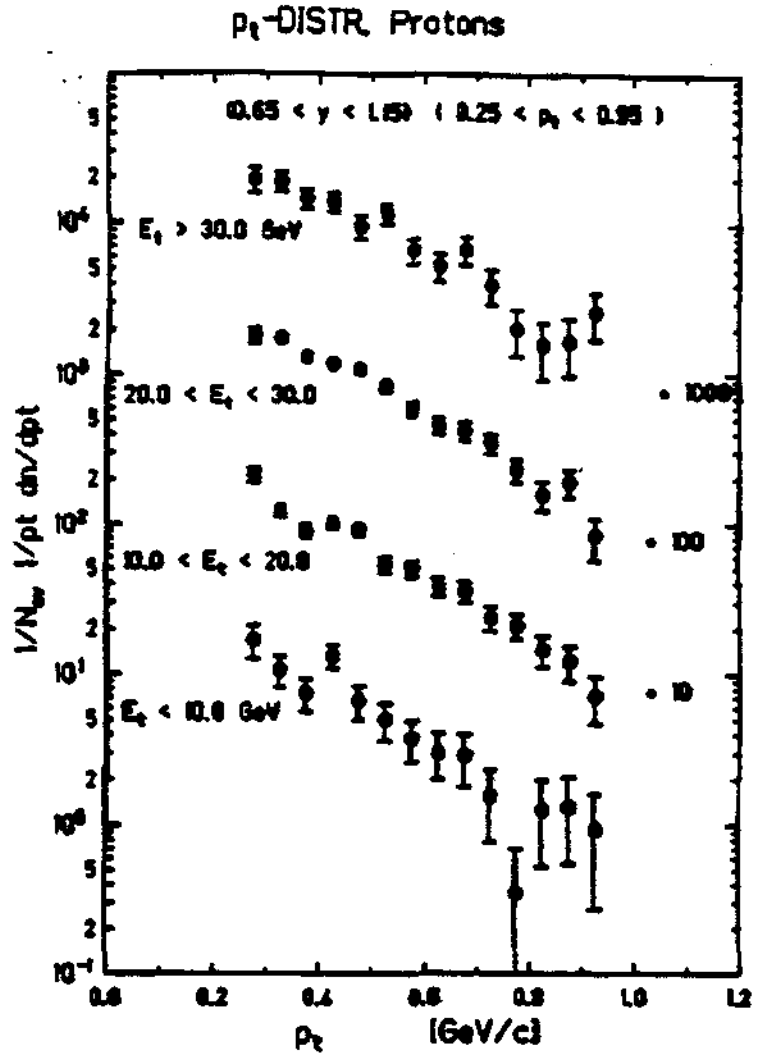

Figure 43: Transverse momentum distributions for p + W → p + X

Chapter 10

Photons and dimuons

10.1 Introduction

The study of real and virtual direct photon production in heavy ion collisions is motivated by the search for thermal radiation from the system formed in the nucleon − nucleon collisions, e.g. a quark gluon plasma [2]. They provide a better measure than hadrons of the "source" temperature, determined by the transverse momentum or transverse mass ($\equiv\sqrt{(p_T^2+M^2)}$) distribution, since they escape the collision unaffected by final state interactions or fragmentation processes.

If the source is thermalized, the resulting distribution is given by $dN/dX_T^2 \sim X_T\, K_1(X_T/T)$ [82], where K_1 is the modified Bessel function, T the temperature and $X_T = p_T$ for photons or M_T the

transverse mass for dileptons. The difference between this expression and an exponential function is only apparent at small X_T/T; with T of the order of 200 MeV, we must measure very low X_T indeed. For dimuons, this requires a measurement near $p_T \simeq 0$.

It has been suggested that the phase transition between hadronic matter and quark matter could be detectable by measuring the production rate of lepton pairs [76][83]. Amongst other features, a square dependence of this rate on particle multiplicity is predicted as one of the signatures for the quark − gluon plasma [84].

A number of experiments with hadron beams have reported observations of a dilepton continuum with masses below the ρ meson [85]. This low mass continuum has been seen both in $\mu^+\mu^-$ and e^+e^- final states, at low (e.g. $\sqrt{s_{pp}} = 5.8$ GeV) and high (e.g. $\sqrt{s_{pp}} = 20.6$ GeV) energy, and with both π and proton beams on relatively light targets (p to ^{12}C). Standard sources, e.g. η Dalitz decays, can only account for about 1/3 − 1/2 of this continuum, and are much less peaked at low x_F.

In addition, in p + p interactions, there is evidence [86] that the rate of low mass e^+e^- pairs, dN_{ee}/dy, is proportional to the square of the associated multiplicity, dN/dy, in a related rapidity interval, y≡arcth(p_L/E). This is a very unusual result, since all known inclusive cross sections (e.g. ρ + X production [87]) scale linearly with the multiplicity.

Thus the major part of the low mass continuum is unexplained and seems to have an unusual multiplicity dependence; we shall call this anomalous continuum production. This anomalous production could be due to annihilation of produced $q-\bar{q}$ pairs into lepton pairs [88] since this mechanism gives a natural explanation of the multiplicity dependence. Our ideas concerning confinement and hadronization would be influenced by a confirmation of this explanation.

For real photons, we concentrate on the comparison of the measured photon p_T spectra with the expected spectra from hadronic sources which were extracted from our measured charged pion p_T spectra. Data from proton, oxygen and sulfur beams at 200 GeV/u with W and Pt targets are compared. Photons are measured via the conversion method in parallel with charged particles in a magnetic spectrometer, spanning an angular range of 15 ° to 45° in θ_{lab}. The main problem in measuring direct photons is the dominance of hadronic sources. Up to several hundred particles, dominantly pions, are created in these collisions [50]. Since the neutral π^0 decays into two photons, one deals with roughly the same number of decay γ's as charged pions. To get a handle on direct photons, a detailed knowledge of the properties of the produced pions is essential.

We also report on the measurement of low transverse mass dimuons in the forward rapidity region in 200 GeV/nucleon ^{32}S interactions, and this will be compared to 200 GeV proton interactions measured in the same apparatus. The major aim is to measure the anomalous production rate and the multiplicity dependence of that production, with the motivation to probe the larger volumes for long hadronization lengths.

For the detailed analysis and other results, see [11] [16] [20] [25].

10.2 Results from external spectrometer on photons

Figure 44 a,b,c show the corrected inclusive p_T spectra for photons observed in p − W, ^{16}O − W and ^{32}S − W(Pt) at 200 GeV/u, respectively. These data are taken in the rapidity range 1.0 < y < 1.9 and the p_T range 0.1 < p_T < 1.5 GeV/c. The full line describes the spectra expected from hadronic sources π^0,η,η',ω. The agreement in shape is remarkable. The π^0 photons serve as normalization.

can be drawn from this, even more since the average absolute value does agree very well with the expectation.

10.3 Results from muon spectrometer on dimuons

10.3.1 Estimation of dimuon background produced in the dump

In chapter 3, we mentioned briefly that the main background in our measurement of low transverse mass dimuons comes from production in the dump. This is shown in Figure 47 and Figure 48 where we have determined the signal, integrated over all masses and, separately, for different mass slices, as a function of Z_{max} after the acceptance correction appropriate to each Z_{max}. We observe that the sulphur data shows a larger Z – dependence than the proton data. In addition, the variation with Z is mass – dependent, larger at low masses but inexistent for masses larger than 1 GeV/c^2. We interpret these variations as due to dimuon production in the dump. We emphasize that the sulphur data includes both fragment and hadron production in the dump while the proton data includes only hadron production in the dump.

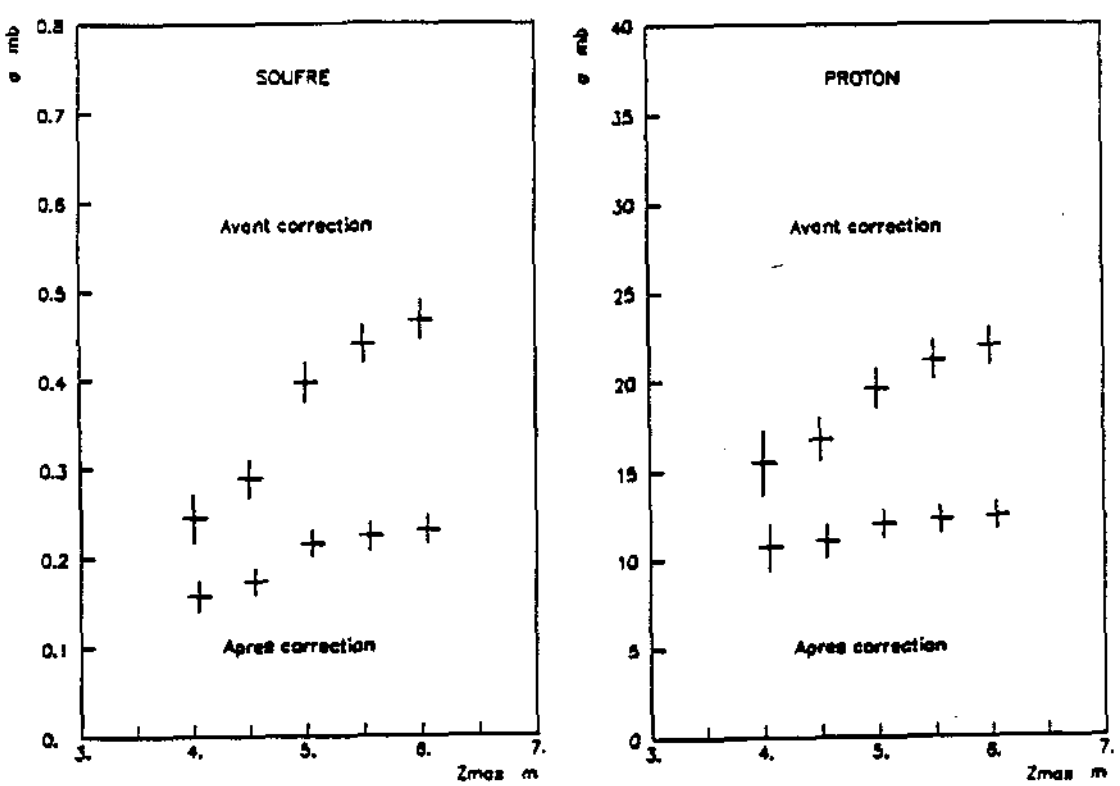

Figure 47: Stability of the integrated distributions as function of the Z_{max} before and after subtraction of the dump production: (a) sulphur and (b) proton.

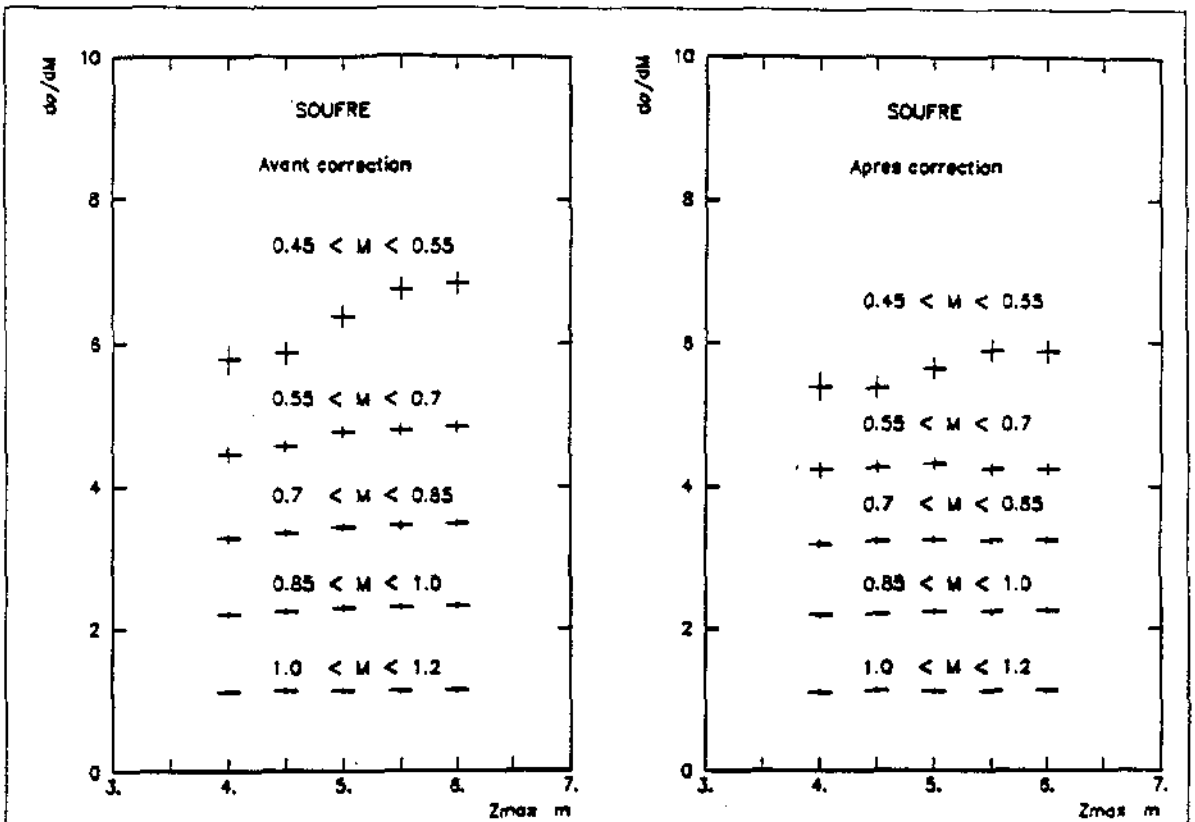

Figure 48: Stability of the sulphur mass distributions as function of the Z_{max} (a) before and (b) after subtraction of the dump production

Our strategy is to simulate the dump background and, within the fixed kinematical region, check the stability of the distributions for different Z_{max} after the acceptance correction and dump background subtraction appropriate to Z_{max}. We have simulated the production of dimuons in the interactions of the produced particles in the dump for both proton and sulphur projectiles. In addition, for sulphur, we have simulated the production of dimuons in the interactions of the beam fragments in the dump and in the subsequent interactions of the particles produced in the fragment interactions; however, the major source of background in the sulphur data is that due to produced particles in the primary interaction. A full simulation of the dimuon production in the full hadronic shower has not been attempted.

In both figures, the distributions are also shown after the subtraction of the dump production, for the sulphur and proton samples. After correction, both samples become somewhat flatter at all masses. In particular, the sulphur sample is flat for M > 0.55 GeV/c^2. Some dump background persists in the lowest mass bin in the sulphur sample. Up to $Z_{max} = 4.5$ for all masses, we understand approximately the dump background in the kinematic region. We estimate the systematic error to be $\pm 15\%$.

See [77] for more details of the simulation of the dump background.

10.3.2 Distributions of mass, rapidity and transverse momentum

For the purposes of this paper, we shall use combined S − Pt and S − Ag data. The average electromagnetic E_T for the combined sample is 90 GeV, where the knee is at about 100 GeV. The distributions of dimuon mass (Figure 49), rapidity (Figure 50) and transverse momentum (Figure 51) are shown for the combined sulphur data, and for the approximately minimum bias p − Pt data corresponding to an average electromagnetic E_T of 2.8 GeV.

10.3.3 Estimation of known sources

The known sources are resonance decays and hadronic bremsstrahlung. The latter is of the order of 10% of the former below the ρ resonance [85]. The resonance decays which are considered are: $\rho,\omega,\phi \to \mu^+\mu^-$, $\eta,\eta' \to \gamma\mu^+\mu^-$ and $\omega \to \pi^0\mu^+\mu^-$.

The resonance production rates, relative to pions, have been measured, usually at high p_T, defined as $(X/\pi^0)_\infty$ where X = meson resonance [78]. The branching ratios are taken from [89], where we have used the better measured e^+e^- ratios in the cases of vector meson decays.

We assume that the ratios $(X/\pi^0)_\infty$ remain the same in nucleus − nucleus interactions as in hadron − hadron interactions. We use the pseudo − rapidity distribution for charged particles as measured in our experiment (see 5.2) from which we deduce the number of π^0/interaction, using $N(\pi^\pm) = 0.92$ N(charged), and $N(\pi^-) = N(\pi^+) = N(\pi^0)$.

We use the cross section for the $< E_T >$ of our samples also determined in our experiment (see 4.2), from which we deduce the dimuon cross section for each resonance.

The X/π ratio as a function of rapidity comes from our measurement of dimuons with $1.0 > M > 0.7$ GeV/c^2, dominated by ρ,ω resonance production. The p_T distribution for the ρ,ω,ϕ,η' resonances is given by [79]:

$$E\frac{d^3\sigma}{dp^3} \propto \left[\frac{2}{(M_T^X + 2)}\right]^{12.3} g(p_T)$$

where $g(p_T)$ does not depend on the mass. The p_T distribution for the η resonance has been measured in the HELIOS/1 experiment [90] and has an additional multiplicative factor relative to [79] for $p_T < 1.25$ GeV/c:

$$h(p_T) = 0.519 + 1.556p_T - 4.393p_T^2 + 2.800p_T^3$$

The decay distributions for the Dalitz decays are taken from [91].

The resulting dimuon distributions are smeared with the experimental resolutions and the same kinematic region is imposed. The results are also shown in Figure 49 − Figure 51.

10.3.4 Anomalous production

The difference between the experimental distributions and those due to known sources is the anomalous production. The results for R_a, the ratio of the dimuon rapidity densities of the data to the known sources in the kinematic region $p_T > 0.2$ GeV/c and $y > 4.1$ are

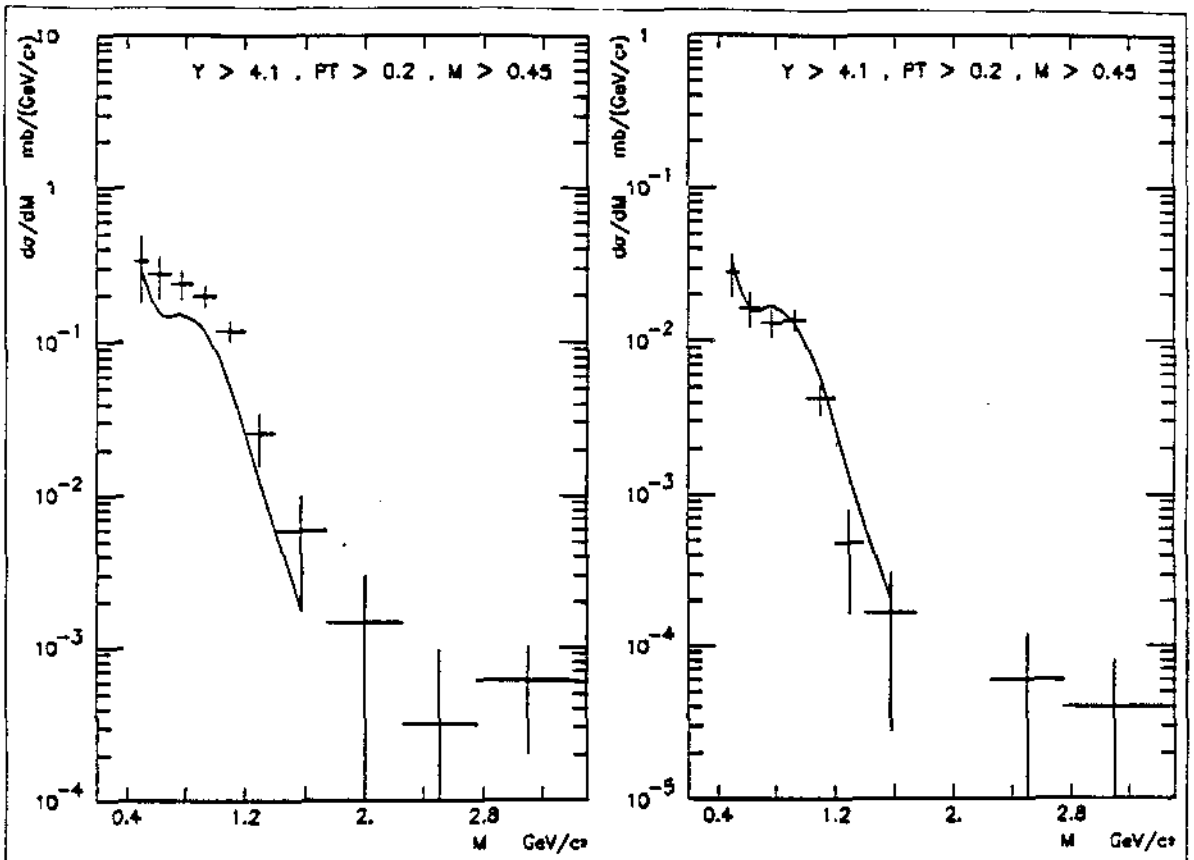

Figure 49: dσ/dM distributions for a) ^{32}S and b) proton interactions

$$(a1)\ R_\mu(S) = 1.41\pm0.37\pm0.78 \quad ; \quad (b1)\ R_\mu(S) = 1.61\pm0.22\pm0.72$$

$$(a2)\ R_\mu(p) = 0.92\pm0.19\pm0.48 \quad ; \quad (b2)\ R_\mu(p) = 0.90\pm0.11\pm0.39$$

where (a) corresponds to $0.45 < M < 0.7$ GeV/c², and (b) to $0.7 < M < 1.0$ GeV/c², and where the first error is statistical and the second systematic.

In each mass region, the results are compatible within the errors with the prediction of the known sources, $R_\mu = 1$. This is expected in the higher mass interval which is dominated by the ρ,ω resonances. However, the proton result in the low mass region is incompatible ($\sim 3.4\sigma$) with $R_\mu \approx 3$, previously measured [85].

10.3.5 Multiplicity dependence

The known sources scale with the multiplicity [87] while anomalous sources have an unknown multiplicity dependence; for a quark−gluon plasma, the expected multiplicity dependence is quadratic, scaled by the number of beam participants to the power 2/3 [84]. For the general case, where ϵ is the fraction of anomalous production, the multiplicity dependence of the measured dimuon cross section, in a given kinematic region and normalized by the measured multiplicity and the total cross section, is

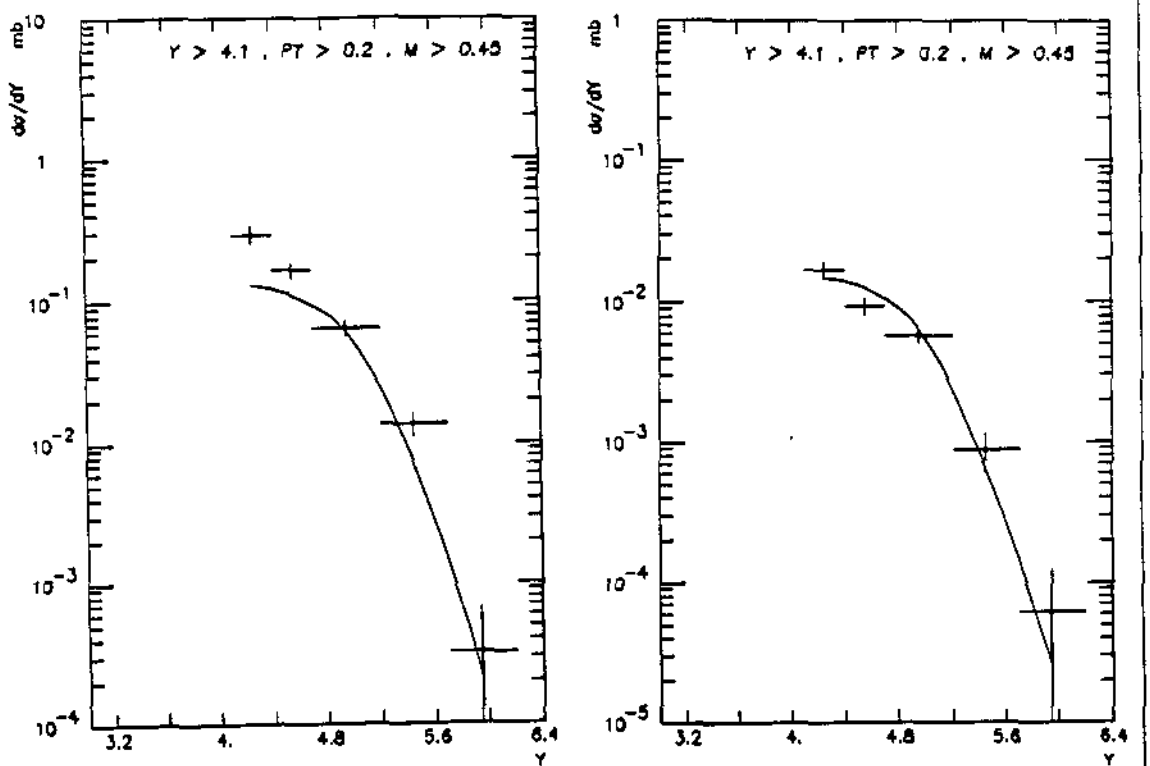

Figure 50: dσ/dy distributions for a) ^{32}S and b) proton interactions. Only statistical errors are shown.

$$R_N = (1-\varepsilon) + \varepsilon N/B^{2/3},$$

where B is the number of beam participants. For our sample of sulphur interactions, the number of beam participants is 28.4 on average; for protons, this is 1, of course.

Using the fits for dN/dη given in 5.2, we have determined the multiplicity in the muon acceptance for SA and pPt:

$$N(S) = 76.4 \pm 13.1$$

$$N(p) = 2.40 \pm 0.45$$

$$\frac{N(S)}{N(p)} = 31.8 \pm 6.6$$

where the error is mostly systematic. In the ratio of the sulphur result to the proton result, some systematic errors cancel.

The experimental ratio in the $0.45 < M < 0.7$ GeV/c^2 mass region is

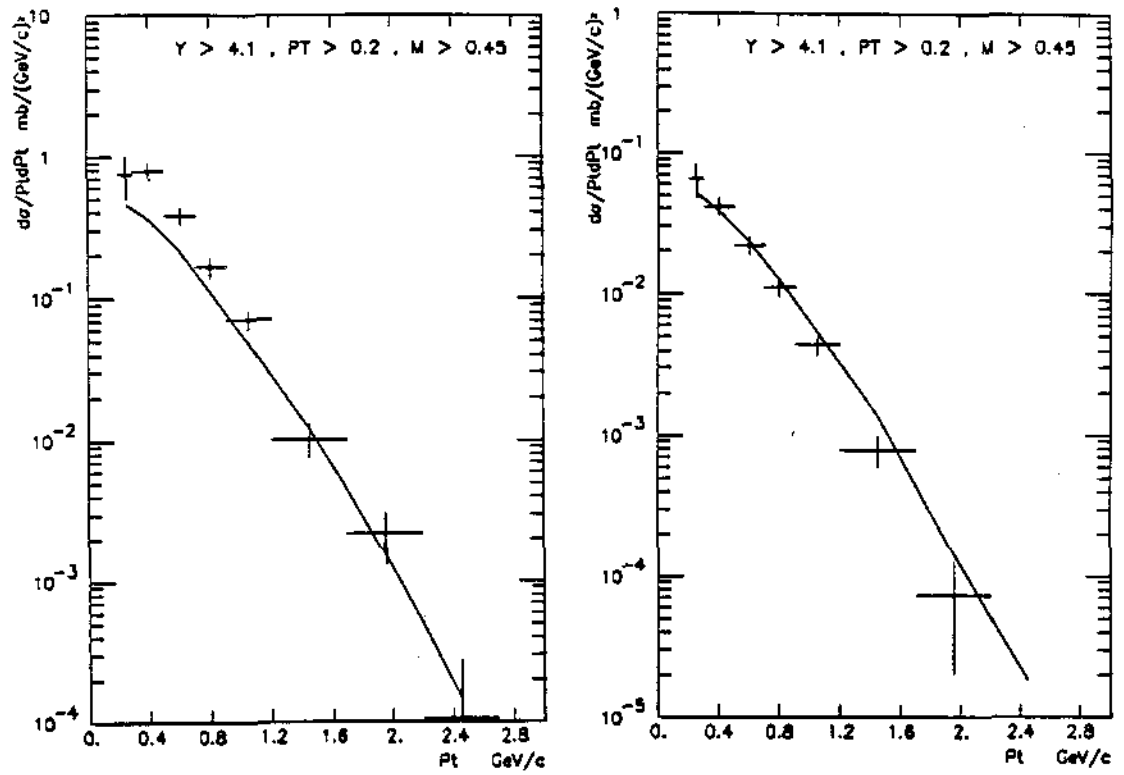

Figure 51: $d\sigma/dp_T$ distributions for a) ^{32}S and b) proton interactions. Only statistical errors are shown.

$$R_N(S)/R_N(p) = 1.64 \pm 0.26 \pm 0.50$$

From these results, the anomalous sources scale with the multiplicity ($\varepsilon = 0$) or the squared multiplicity ($\varepsilon = 1$) within 1.1σ and 3.3σ, respectively, for the low mass kinematic region where we have combined the statistical and systematic errors quadratically.

Similar results are obtained in other kinematic regions ($0.7 < M < 1.0$ GeV/c^2, $0.2 < p_T < 0.7$ GeV/c, $0.7 < p_T$, $4.1 < y < 4.7$ and $4.7 < y$) and in a "central" region ($0.45 < M < 0.7$ GeV/c^2 and $0.2 < p_T < 0.7$ GeV/c and $4.1 < y < 4.7$).

10.4 Discussion

There are no unusual effects seen neither in direct photons nor in dimuons; however the errors, especially in the latter case, are quite large.

The p_T spectra of photons were measured for p – W, ^{16}O – W and ^{32}S – W(Pt) at 200 GeV/u. Within the statistical (4% – 11%) and systematic errors (9%) these spectra agree in shape and absolute cross section with the expected photon spectra from hadronic sources, which has also uncertainties of about 9%, mainly due to lack of knowledge about η production.

We have made a measurement of low transverse mass dimuons in the forward rapidity region in 200 GeV/nucleon ^{32}S interactions with nuclei, and have compared this measurement with that in the same apparatus in 200 GeV/c proton interactions. The results in both cases are consistent with no "anomalous" low mass dimuon production, but have large statistical and systematic errors. In both proton and sulphur interactions, the low mass and $\rho + \omega$ regions give similar results relative to known sources. The increase in low mass dimuon production from proton to sulphur interactions is consistent within the large errors with the increase in the charged multiplicity in the same kinematic region.

Dimuon error analysis for Madrid contribution

Georges London and Georges Vasseur
DPhPE, Saclay

HELIOS NOTE 429

Chapter 1

Introduction

We present the muon error analysis used in the contribution to the Madrid conference and in G.Vasseur's thesis [1]. We indicate where this can be improved. A new estimate is made of the upper limit on a dimuon source with a quadratic multiplicity dependence. We also try to estimate the situation for NA34/3 in order to pinpoint the improvements, etc.

Chapter 2

Dimuon Signal

From the samples of good two-muon events with all charge combinations (N^{++}, N^{+-}, N^{--}), we first subtract the combinatorial background, then correct for the geometrical acceptance (including the Zcut) and, finally, subtract the dump background.

2.1 Statistical errors

To improve our knowledge of the shape of the like-sign subtraction in any given variable, we make a large sample of false + − combinations from our samples of like-sign dimuons, applying only the hodoscope trigger requirement that the two tracks do not hit the same slab. The fraction of false combinations in the i^{th} bin, x_i, is then known to arbitrarily high accuracy.

We perform the like-sign subtraction in the i^{th} bin by using the number of + − events in that bin, N_i^{+-}, x_i and the number of like-sign pairs in our entire sample, N^{++} and N^{--}; the subtraction to obtain the unlike signal from any source and its variance for a very large number of false combinations are as follows:

$$S_i'' = N_i^{+-} - 2x_i\sqrt{N^{++}N^{--}}$$

$$\sigma_i^2 \approx N_i^{+-} + x_i^2(N^{++} + N^{--})$$

The detailed Monte Carlo of the dump background gives the ratio of dump background to signal from the target in any kinematical bin, i; let us define this as $(D/S)_i \equiv f_i$. This enables us to get the signal from the target: $S_i = S_i''/(1 + f_i)$. The error due to this correction is estimated below in the systematic errors on the signal.

We shall take, as a numerical example, the lowest mass bin in our analysis, $0.45 < M < 0.55$ GeV/c^2, where the numbers for sulphur ($N_i^{+-} = 669$, $N^{++} = 1084$, $N^{--} = 977$, $x_i = 0.22$ and $f_i = 1.6$) lead to a signal of 86 ± 11, or 13% statistical error, comparable to the systematic error on the signal in this bin, see next section. For protons, the numbers ($N_i^{+-} = 78$, $N^{++} = 9$, $N^{--} = 4$, $x_i = 0.24$ and $f_i = 1.2$) lead to a signal of 35 ± 4, or 12% statistical error. Notice that since the like-sign subtraction is considerably smaller, the relative statistical error for the proton data is about the same with 8.5 less unlike-sign pairs. Thus, for the same statistical accuracy, the sulphur data should be about 14x the proton data, taking into account the like-sign pairs.

For NA34/3 and the same target – to – absorber distance (i.e. the same decay probabilities), the expected increase of 50x in the statistics reduces the error in any bin by about 7, and in the examples above, to about 2% in both cases.

2.2 Systematic errors on the signal

2.2.1 Global errors

An overall normalization error of 10% has been estimated. This includes the error in the various efficiencies, i.e. in the hodoscope trigger, chamber trigger and MUREC. The product of these efficiencies is about independent of any given variable, e.g. the dimuon mass, and can be assimilated to an overall correction.

2.2.2 Point – to – point errors

1. The acceptance corrections, including that of the Z – cut, have been determined with a simplified Monte Carlo. This has been checked at a few points with a full GEANT simulation and gives errors of $\pm 10\%$.

2. The dimuon decay distribution was isotropic in the simulation. An average 15% decrease in the acceptance is calculated if one uses the $1 + \cos^2\theta$ distribution. We should probably treat this by taking the average value in each bin between the two extreme cases. On average this would give a $\pm 7.5\%$ correction, which in reality varies point – to – point. This problem should be investigated further by looking at what limits data give to the A coefficient in a $1 + A\cos^2\theta$ distribution.

3. The dump subtraction comes from a Monte Carlo simulation of the ratio, Dump/Signal≡f, which depends on the Z – cut [2]. For Sulphur interactions at a Z – cut of 4.5 m and for all masses, this ratio is 0.67 of which 20% are due to fragments; for proton interactions, it is 0.53. From varying the many parameters in the simulation, an estimate of $\pm 15\%$ was made on the ratio. This leads to a $\pm 5 - 6\%$ error in the signal after subtraction. In the lowest mass bin, this error is $\pm 9\%$.

It is clear that the reliability of the latter result would be greatly improved by a few special runs during the present 1989 run in which we would send beams directly into the DLAC and trigger normally on di – muons. These kind of runs are forseen for NA34/3.

Chapter 3

Estimation of known dimuon sources, with systematic errors

3.1 Estimation

The known sources which have been considered are the Dalitz decays of the η, η' and ω mesons, and the dimuon decays of the ρ, ω and ϕ mesons. We have determined the cross section for each of these mesons, called generically X, by relating to the π^0 cross section, using the following equations:

$$\sigma_X = \sigma_{tot}(N_{ch}/interaction)(N_{\pi ch}/N_{ch})(N_{\pi 0}/N_{\pi ch})(N_X/N_{\pi 0}) \equiv E_0\, E_1\, E_2\, E_3\, R_X$$

We assume that all cross sections factorize in p_T and η:

$$\frac{d^2\sigma}{dp_T d\eta} = A f(p_T) g(\eta) \text{ where } \int g(\eta) d\eta = 1$$

The ratio of X mesons to π^0 mesons is therefore

$$R_X = \frac{A_x \int f_x(p_T) dp_T}{A_\pi \int f_\pi(p_T) dp_T}$$

As p_T gets very large, the ratio of the integrals becomes 1, and A_X/A_π becomes a constant, defined as $(X/\pi^0)_\infty \equiv E_4$, as measured in many experiments.

The numbers E_i are taken from experiment. E_0 comes from [3] for protons and from our E_T measurement for sulphur; the respective errors are 7% and 11%. E_1 comes from the Gaussian fit to the silicon ring measurement [4]; the errors used are 17% for sulphur and 19% for proton. These are probably overestimates which our Torino colleagues will correct. E_2 is 0.92±0.2 and $E_3 = 1/2$. The latter number is somewhat underestimated due to decays such as $\eta \Rightarrow 3\pi^0$.

The errors on E_4 are 11% for the η',ρ,ω and 20% for the ϕ; the error for the η is only 3% [5]. We shall see shortly that this latter error is overshadowed by the imprecision of our knowledge about the transverse momentum shape. The η' error should be 30% unless improved by NA34/1.

The other number needed from experiment is the branching ratio of the X meson into a dimuon, which we will call E_5. The errors used are 3 – 5% for (ρ,ω,$\phi \Rightarrow$ee) and (13,20,27)% for the (η,ω,η') Dalitz decays [6]. The values using the ee decay mode should be corrected for the threshold factor when going to $\mu\mu$.

To know what fraction of σ_X is accepted within our cuts ($M > 0.45$ GeV/c^2, $p_T > 0.2$ GeV/c and $y > 4.1$), we need to know the functional forms of $f(p_T)$ and $g(\eta)$. For the transverse momentum dependence, we have used [7]

$$f(p_T) = 2p_T \left[\frac{2}{(M_T^X + 2)} \right]^{12.3} h(p_T)$$

where

$$h(p_T) = \exp(-p_T) \text{ if } p_T \leq 1 GeV/c \quad \text{or} \quad \exp\left[-\frac{23(p_T - 1)}{\sqrt{s}} - 1 \right] \text{ if } p_T \geq 1 GeV/c$$

This has been modified for the η meson for $p_T < 1.25$ GeV/c by [8]

$$0.519 + 1.556 p_T - 4.393 p_T^2 + 2.800 p_T^3$$

For the η meson, the shape at small p_T is only known to about 20% which is the error we have used. For the other mesons, we have tried a different shape, $f(p_T) = p_T \exp(-6.4\ M_T)$ [9] which gives a 25% error. NA34/1 should improve matters at least for the $\rho + \omega$.

For the rapidity dependence, we have used the charged particle distribution as determined by the Si rings modified for $y > 4.8$ by

$exp(-12(y-4.8)^2)$

as determined by the dimuon rapidity distribution with $0.7 < M < 1.0$ GeV/c^2 in the proton sample, dominated by ρ and ω mesons. If we use the rapidity dependence of [7], which however does not fit our data, the known sources increase by 25%. We thus, somewhat arbitrarily, assign a $\pm 25\%$ error due to our lack of knowledge. We should use our data to set limits. This uncertainty should be greatly improved by NA34/1.

The decay distributions are Breit−Wigner functions for $\rho,\omega,\phi \Rightarrow \mu\mu$ and Kroll−Wada [10] for the Dalitz decays. The resolutions are folded in.

The errors are summarized in Table 1. The overall error due to the lack of knowledge of the known sources is about 40%! The major errors are due to our measured $dN_{ch}/d\eta$ (probable overestimate) and to the p_T and y dependence. It will be hard to reduce this overall error below 25−30%.

Table 1: Summary of systematic errors concerning the known sources

description	sulphur error (%)	proton error (%)
σ_{tot}	11	7
N_{ch}/int	17	19
$N_{\pi ch}/N_{ch}$	2	2
$N_{\pi 0}/N_{\pi ch}$	0	0
$N_{\eta}/N_{\pi 0}$	3	3
$BR(\eta \Rightarrow \mu\mu\gamma)$	13	13
η p_T dependence	20	20
X rapidity dependence	25	25

3.2 Some results

For completeness, we include some results.

We divide the dimuon mass region in two regions, low mass ($0.45 < M < 0.7$ GeV/c^2) and $\rho+\omega$ mass ($0.7 < M < 1.0$ GeV/c^2), and determine the ratio of the signal to the known sources. See Table 2. Upper limits can be given to anomalous production relative to known sources from these numbers.

Table 2: Ratio of signal to known sources

mass region	sulphur	proton
low	1.41±0.17±0.57	0.91±0.10±0.37
ρ+ω	1.61±0.16±0.67	0.90±0.09±0.37

Chapter 4

Multiplicity dependence of dimuon signal

As far as we know, the known sources of dimuons vary linearly with the multiplicity measured in the same rapidity interval, dN/dy. An anomalous signal could vary quadratically with this rapidity density, normalized by the number of projectile participants to the 2/3 power [11]. Using the quadratic dependence as a signature of anomalous production, we do not have to determine the known sources, eliminating many systematic errors.

4.1 Ratio of sulphur to proton data

4.1.1 Normalization of each mass bin to σ_{tot} and N_{ch}

For each projectile, we have normalized the dimuon cross section by the total cross section and the charged multiplicity in the muon acceptance, giving $R_N(S)$ and $R_N(p)$. We do not invoke an estimation of the known sources.

In the ratio, $R_N(S)/R_N(p)$, there is some cancellation of systematic errors. The remaining systematic errors are relative between sulphur and proton runs: normalization, dump subtraction, charged multiplicity and cross section. For the moment, we have assumed no correlation between these evaluations for the two projectiles, and have used the numbers given in the previous chapter.

For the quadratic dependence, one must use $(dN/dy)^2/P^{2/3}$, where P is the number of participating projectile nucleons. For protons, P is obviously 1; for our sulphur sample, P = 28.4. No error has yet been evaluated for the latter number. For pure quadratic dependence, the charged multiplicity ratio of 31.8 becomes 3.5 when normalized by $P^{2/3}$.

The ratio varies from 1 to 3.5 for the two extreme situations. It can be compared to the results in Table 3; nothing can be concluded.

Table 3: Each signal normalized to total cross section and charged multiplicity

mass region	sulphur/proton
low	1.64±0.26±0.50
ρ+ω	1.90±0.27±0.54

4.1.2 Normalization of the lowest mass bin by the "$\rho + \omega$" bin

We treat the systematic errors better if we normalize the low mass region by the $\rho + \omega$ region. This was not done for the Madrid contribution, but has been since. There is a different cancellation of systematic errors to be considered. This method becomes more easily interpretable when the resonance peak is more pronounced, as in NA34/3.

For each projectile, we determine the ratio of dimuon yield for $0.45 < M < 0.7$ GeV/c^2 relative to that for $0.7 < M < 1.0$ GeV/c^2. The only remaining systematic error is due to the relative error in the dump subtraction. For the moment we have used an independent systematic error for each projectile. See Table 4.

Table 4: Low mass region normalized to $\rho + \omega$ region

sulphur	proton	sulphur/proton≡R
1.14±0.18±0.10	1.32±0.20±0.11	0.86±0.19±0.10

The ratio of ratios, R, is of order 1, indicating that the low mass region behaves the same relative to the $\rho + \omega$ region in both proton and sulphur interactions. However, the errors are large, with the statistical errors greater than the systematic.

We attempt to place a quantitative limit on a dimuon source with a quadratic multiplicity dependence. We assume that the $\rho + \omega$ region has a linear multiplicity dependence and that the low mass region has an unknown admixture of linear and quadratic terms, $\propto$ to $dN/dy + \lambda(dN/dy)^2/P^{2/3}$. R is related to λ:

$$R = \frac{1 + \lambda(dN/dy)_S/P^{2/3}}{1 + \lambda'(dN/dy)_p} \equiv \frac{1 + \lambda(dN/dy)_S/P^{2/3}}{1 + k\lambda(dN/dy)_p}$$

where $\lambda' \equiv k\lambda$. We determine the fraction, f, of dimuons produced by quadratic processes in the low mass region in sulphur interactions:

$$f \equiv \frac{\lambda(dN/dy)_S/P^{2/3}}{1 + \lambda(dN/dy)_S/P^{2/3}} = \frac{R - 1}{R[1 - kP^{2/3}(dN/dy)_p/(dN/dy)_S]}$$

For values of k between 0 (no quadratic dependence in proton interactions) and 1 (same quadratic dependence in protons as in sulphur), the 90% confidence upper limits on f vary between 0.3 and 0.4. With reduced errors in NA34/3, this should be a powerful method for determining limits on collective behavior.

4.2 E_T dependence for a given projectile

This has not yet been done, but there is another cancellation of systematic errors to be considered.

In particular in the ratio of samples for two different E_T bins in the same run, the remaining systematic errors are those due to the relative normalization (problem of connecting two triggers with two thresholds) and the dump subtraction. However, it should be noted that the signal/dump estimate is approximately independent of E_T and that, in the ratio, there are many cancellations of unknowns. The error has not yet been evaluated; it will be determined largely by our special runs.

Note that the charged multiplicity ratio, e.g. between $E_T^{HLACEM} = 50$ and 120 GeV, is only 1.6, with the number of participating projectile nucleons = 22 and 32, respectively. For pure quadratic dependence, the relevant ratio is only 1.3.

4.3 Trigger influence on the N_{ch} dependence for a given projectile

This can not be done in NA34/2 but can be in NA34/3.

We need to determine the ratio of the numbers, with and without a dimuon trigger requirement, of the events with the same charged multiplicity vs N_{ch}. This can be done by dimuon kinematic region. The absolute value is of no interest, only the slope. The only systematic error which influences this ratio is the dump subtraction but, since this is approximately independent of E_T or N_{ch}, the slope is unaffected to first order.

We must take data in NA34/3 without the dimuon trigger.

References

1. G.Vasseur, *These de Doctorat de l'Universite Paris 11 (1989)*
2. A.Gaidot, *NA34/3 note 4 – bis*
3. A.S.Carroll et al, *Phys.Lett. 80B (1979) 319*
4. M.Masera, *HELIOS note 401*
5. for example, A.Chilingarov et al., *Nucl.Phys. B151 (1979) 29: $\rho/\pi,\phi/\pi$;* C.Kourkoumelis et al., *Phys.Lett. 84B (1979) 39: η/π;* M.Diakonou et al., *Phys.Lett. 89B (1980) 432: $\omega/\pi,\eta'/\pi$.*
6. Particle Data Group, *Phys.Lett. B204 (1988) 1*
7. M.Bourquin and J. – M.Gaillard, *Nucl. Phys. B114 (1976) 334;* example of M_T scaling for ρ/π in [9]
8. HELIOS note 416
9. T.Akesson et al., *Nucl.Phys. B203 (1982) 27*
10. N.M.Kroll and W.Wada, *Phys.Rev. (1955) 1385;* note that some errors have been corrected, A.Gaidot, *private communication*
11. for example, R.C.Hwa and K.Kajantie, *Phys.Rev. D32 (1985) 1109*